International Research Journal of Engineering and Technology (IRJET) e-ISSN: 2395-0056
Volume: 10 Issue: 06 | Jun 2023 www.irjet.net p-ISSN: 2395-0072

Design of Integrated Generator-Rectifier System to Determine the Maximum Power Point Tracking of Wind Turbine.

J. Mahadeshwan Nayak*, Dr. M. Sushama**

**(M. Tech, Department of Electrical Engineering, JNTUH University College of Engineering, Hyderabad, India,*
***(Professor, Department of Electrical Engineering, JNTUH University College of Engineering, Hyderabad, India,*

Abstract - *Offshore wind turbines are widely favored for their higher energy generation capabilities compared to onshore turbines. Additionally, they support good weather and aquatic conditions. The need for effective power conversion technologies makes it difficult to meet an aggressive Levelized Cost of Energy (LCOE) objective for offshore turbines. A combination system that combines a Permanent Magnet Synchronous Generator (PMSG) with a rectifier system can be used to overcome this problem. An active rectifier and numerous passive rectifiers make up the rectifier system. However, obtaining the requisite maximum power output is challenging due to the presence of uncontrollable passive rectifiers. This research suggests a unique Fuzzy Logic Controller (FLC)-based Maximum Power Point Tracking (MPPT) architecture to address this problem. The proposed method enables the acquisition of maximum power (MPPT) by using FLC to analyze the d-axis current generated. Utilizing MATLAB/Simulink, the proposed method's efficacy is assessed.*

Key words: FLC, MPPT, Rectifiers, and Offshore Wind Turbines

1. INTRODUCTION

The movement of air or gases from one place to another that results from variations in pressure and temperature is known as wind. Utilising these winds successfully allows for the production of wind energy. Modern methods for harnessing wind energy as electricity have been introduced in recent years. Depending on the region, there are two types of wind energy: onshore wind energy and offshore wind energy. Onshore wind energy involves producing electricity from wind turbines that are situated on land. On the other side, offshore wind energy is produced by wind that travels across the ocean. Typically, offshore wind energy is created in the ocean.

Wind energy is a clean, renewable energy source that has a lot of potential for diversifying the world's electricity supply. It is increasingly being used as a renewable energy source. In comparison to onshore wind energy, offshore wind energy offers the advantage of a more reliable and powerful wind spectrum. Furthermore, because offshore winds are milder, turbine fatigue is reduced and its usable life is increased. The great potential of this renewable energy source is demonstrated by the increasing installed capacity of offshore wind turbines. Offshore wind turbines can now generate electricity at a levelized cost that is competitive with onshore alternatives.

The power outputs of the Gamesa10X [3] and Halide X [4] wind turbines are around 10–12 MW. The constraints of present converter topologies make it difficult to create dependable electromechanical power conversion systems for these high-power-density, energy-efficient turbines. The primary difficulties are brought on by power electronics switches' low voltage/current ratings and increasing switching losses [5]. Currently, two-level pulse width modulation (PWM) and neutral-point-clamped converters are frequently used. The second strategy is chosen because it provides a most simple design and operating approach.

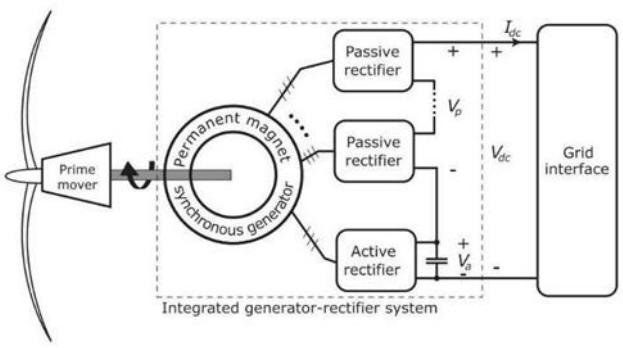

Fig.1. Architecture for tracking the power points.

The architecture for tracking power points comprises connecting power electronic devices in series and/or parallel to manage many megawatts of power. However, the unequal distribution of losses across the switches in these configurations makes them frequently unreliable, which increases failure in hotspot locations. A neutral-point-clamped topology is used to solve this problem, greatly reducing the peak voltage that may be delivered to each switch [6].

Reducing the power rating of individual power converters is the goal of implementing a multiport generator. Utilizing just active rectifiers, which convert AC to DC, is one strategy. Permanent magnet synchronous generators (PMSGs)-based integrated generator-rectifier systems are a possibility, as depicted in Fig. 1 [7]. Rectifiers fitted to each port in

multiport PMSGs transform the kinetic energy from the turbine shaft's rotation into alternating current power. A high-voltage direct current (DC) bus is built by joining the rectifier outputs in series. In this design, just a small portion of the entire voltage on the DC bus is present across each rectifier. A viable alternative is the combined generator-rectifier system based on a permanent magnet synchronous generator (PMSG), as shown in Fig. 1 [20], [21]. In this system, a multiport PMSG transforms the mechanical energy from the turbine shaft into AC electrical energy. For the conversion of AC to DC, a passive or active rectifier is attached to each port of the PMSG. A reasonably high-voltage DC bus is created by series-connecting the rectifiers' DC outputs. Only a small percentage of the overall DC-bus voltage is handled by each rectifier. Passive rectifiers process 60% of the total power as a result, which, under rated working conditions, results in a 47% reduction in conversion loss. The active rectifier's size has been decreased, which has enhanced the system's overall power density and dependability.

It is suggested that a control framework be used to achieve maximum power point tracking (MPPT) by establishing a link between the total DC power and the active rectifier's d-axis current. The use of uncontrolled passive rectifiers is replaced by this control system. To accomplish maximum power point tracking (MPPT) and enhance the effectiveness of wind energy conversion systems, a controlled framework is introduced. In this framework, fuzzy logic (FL) controllers are used to analyze the d-axis current of the active rectifier. FLC offers an inference mechanism that delivers flexible values for accomplishing MPPT in contrast to conventional Proportional-Integral (PI) controllers with constant values. This makes it possible to generate more electricity and more precisely capture all of the wind energy that is present. An advantageous option for wind power applications, the integrated rectifier system utilizing FLC contributes to a competitive levelized cost of energy (LCOE). Three sections make up the paper. The MPPT-based power flow regulation for a combined generator-rectifier system is covered in Section II. The simulation findings in Section III show how successful the suggested control strategy is. Section IV, which summarizes the results and discusses potential future study options, brings the paper to a close.

2. The Integrated Generator-Rectifier System's Power Flow:

A framework for controlling the power flow in the combined generator-rectifier system has been created during this stage. assuming that a hard-wired connection connects the system's DC output to a DC grid interface. This presumption has been shown to be true for both AC and DC grids [5]. The converter on the grid side of an AC grid controls the DC bus, which acts as an interface. In contrast, the DC side grid converter in a DC grid is in charge of managing the DC voltage [9].

A simplified version of the equivalent circuit for the generator-rectifier system is shown in Fig. 2. In the combined generator-rectifier system, Vp stands for the voltage generated by the passive rectifiers. The generator's rotational speed and this voltage are directly inversely related. An Xp-valued commutation reactance is linked in series with a Vp-valued voltage divider to reduce the output voltage ripples of the passive rectifiers. It is possible to effectively disregard the overall ripples in the output voltage of the passive rectifier by maintaining a phase shift between various AC ports.

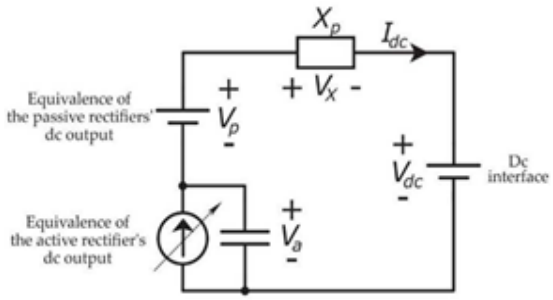

Fig.2. represents a general circuit of the combined generator-rectifier system.

By deducting the output voltage of the passive rectifier, Vp, from the constant grid interface voltage, one may calculate the DC-side voltage of the active rectifier, denoted as Va. The active rectifier extracts controllable power from the system in the form of a controllable current source. The current on the DC-side is represented by this controlled power. The current obtained from the active rectifier determines the total power flow into the DC bus due to the series connection.

3. Minimization of Voltage Ripple in Passive Rectifier:

Considering a total of k three-phase AC ports, the passive rectifiers for a PMSG are fed via (k - 1) ports without output filter capacitors. Every π/3 radian, the voltage ripple peaks. The DC outputs can be linked in series with an appropriate phase shift of π/3(k-1) radians to lessen voltage ripples. When (k - 1) passive rectifiers with a phase shift of π/3(k-1) radians are used in a system, the voltage ripple is decreased.

It is possible to attain the DC output voltage of (k-1) passive rectifiers at frequency Idc by taking into account a constant DC bus current and little voltage ripple. It is important to note that a rise in the number of AC ports decreases voltage ripples, albeit at a slower rate. A similar strategy is used to employ phase shifting transformers and multi-pulse diode rectifiers to further reduce harmonic distortion in high-power drives. The phase current commutation switching

period is estimated to be less than one-sixth of the entire time length due to the assumption that the synchronous inductance, represented as "L," is relatively small. This circumstance is equivalent to a conventional six-pulse diode bridge rectifier operating in the first mode. The comparable series resistance for each port per phase is denoted by the letter "R." Electrical frequency affects the back electromotive force, or E(w).

$$E(\omega) = \frac{\omega}{2\pi f_0} E_0$$

At the output DC side voltage of the passive rectifier, the resistance per phase, synchronous inductance, and DC bus current are collectively referred to as Vx. It is affected by the back electromotive force (EMF), which is represented by Eo and is the rated line-to-neutral peak of each alternating current port, as well as the rated electrical frequency (fo) of each AC port.

4. Power-Flow Control Using Active Rectifiers:

It is done to calculate the DC bus power from the active rectifier's AC side current. The active rectifier's conversion losses are not taken into account in this computation. Both the AC and DC sides have equal power.

$$\frac{3}{2}E(\omega)I_{sd} - \frac{3}{2}I_{sd}^2 R = V_a I_{\mathrm{dc}}$$

Va stands for the active rectifier's dc-side voltage, while Isd stands for the AC side's d-axis current component. It is crucial to understand that phase-A's greatest back electromotive force (EMF) lines up with the d-axis.

Va = Vdc - Vp + Xp * Idc

In this equation:

- Va represents the dc-side voltage of the active rectifier.
- Vdc represents the dc voltage.
- Vp represents the voltage drop.
- Xp represents the reactance.
- Idc represents the dc current.

Current of dc current is given by

$$I_{\mathrm{dc}} = \frac{P_{\mathrm{dc}}}{V_{\mathrm{dc}}}$$

The equation demonstrates how equations (4) and (5) can be added to equation (1) to produce the power at the DC bus. The d-axis current of the active rectifier and the power at the DC bus are significantly correlated.

$$\frac{3}{2}E(\omega)I_{sd} - \frac{3}{2}I_{sd}^2 R = P_{\mathrm{dc}}^2\left((k-1)\frac{1}{V_{\mathrm{dc}}^2}\left(\frac{3}{\pi}\omega L + 2R\right)\right) + P_{\mathrm{dc}}\left(1 - \frac{3}{\pi}(k-1)\frac{\sqrt{3}E(\omega)}{V_{\mathrm{dc}}}\right).$$

It can be seen from the previously described equation (6) that the active rectifier's d-axis current significantly affects the regulation of the DC-bus power. The power drawn from the turbine can be regulated equivalently by altering the d-axis current. In other words, controlling the d-axis current enables efficient control of the turbine's power flow and utilization.

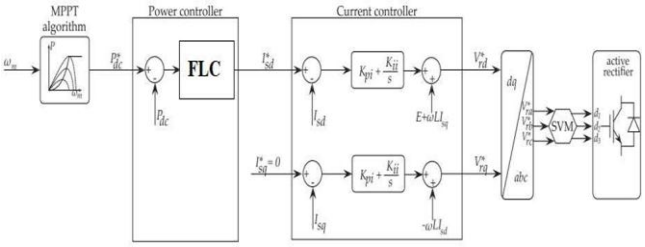

Fig 3. Block Diagram of Power Flow Control

Figure 3's depiction of the cascade design is used to control the power flow. The active rectifiers' d-axis and q-axis currents are controlled by current controllers in the inner loop. The q-axis current regulates the power factor whereas the d-axis current controls the power flow. The fuzzy logic controller (FLC) used by the outer loop power controller modifies the d-axis current signal in order to send the desired reference power (P*dc) to the DC-bus. The generator's rotational speed serves as the FLC's input, and the MPPT algorithm generates the power signal. The active rectifier obtains a power factor of 1 at no current on the q-axis. The dynamics of the AC current at the port in the reference frame can be used to model the current controllers. The specific control method and design selected for the current controllers will determine the modelling equations.

$$L\frac{dI_{sd}}{dt} = -RI_{sd} + \omega LI_{sq} + E - V_{rd} \text{ and}$$

$$L\frac{dI_{sq}}{dt} = -RI_{sq} - \omega LI_{sd} - V_{rq}$$

In the example, Vrd and Vrq stand for the input d-axis voltage and q-axis current, respectively. In phase-A, the d-axis aligns with the maximal back electromotive force (EMF), and the q-axis is 90 degrees in front of the d-axis. A PI (proportional-integral) controller that integrates feed-forward terms to produce voltage along the d-axis is implemented using equation (7).

$$V_{rd}^{*} = K_{pi}(I_{sd}^{*} - I_{sd}) + \int K_{ii}(I_{sd}^{*} - I_{sd})dt + E + \omega_0 L I_{sq}$$

Equation (8), which is the same method used for the d-axis current controller, can be utilised to create the q-axis current controller. With respect to the q-axis reference current I*qs, Kpq stands for the proportional gain and Kiq for the integral gain in Equation (8). Equation (6) uses the known values of L (inductance) and R (resistance) to directly calculate the power demand based on the d-axis current command. Parametric uncertainty in power flow control is decreased through the implementation of an outer-loop PI control. The above information shows this outer-loop control method.

$$I_{sd}^{*} = K_{pp}(P_{\mathrm{dc}}^{*} - P_{\mathrm{dc}}) + K_{ip}\int (P_{\mathrm{dc}}^{*} - P_{\mathrm{dc}})dt$$

The terms Kpp and Kip stand for the proportional and integral gains, respectively. Based on the difference in inaccuracy between the reference signal and the measured signal, the proportional gain, Kpp, decides how the controller will react. In order to eliminate steady-state errors and regulate the system's responsiveness over time, the integral gain, Kip, is used. The outer-loop PI control may successfully control the power flow and achieve the required system performance by modifying the values of Kpp and Kip.

5. Fuzzy Logic Controller System:

By using a thought process and rule-based techniques, fuzzy logic controllers are in fact regarded as effective tools for boosting the performance of electrical equipment. Fuzzy logic controllers include an inference system that takes into account a variety of feasible values, in contrast to PI controllers where the proportional and integral gain values are fixed. Compared to conventional PI controllers, this dynamic technique enables greater accuracy and better power flow management [10]. The power received through the maximum power point tracking (MPPT) algorithm and the change in power are the two inputs used in the specific instance of the aforementioned fuzzy logic controller. The controller then outputs a signal that modulates the current along the d-axis. In order for the fuzzy logic controller to function, four crucial steps must be completed.

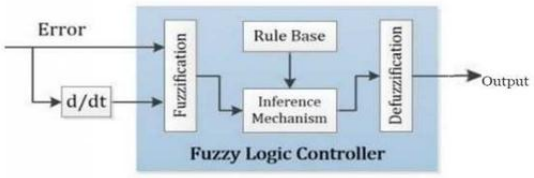

Fig 4. Fuzzy Block Diagram

(i) Fuzzification: Using a collection of membership functions (MFs), crisp values are transformed into fuzzy values in the fuzzification step of the fuzzy logic controller. The membership functions specify the level of a particular input's or output's membership in different fuzzy sets. In this instance, Figures 5, 6, and 7 show, respectively, the membership functions for the power error input, change in power input, and output. The membership functions give the inputs and outputs a linguistic representation, enabling a more flexible and understandable control system. The controller can deal with the uncertainty and imprecision present in real-world systems by fuzzifying the crisp inputs.

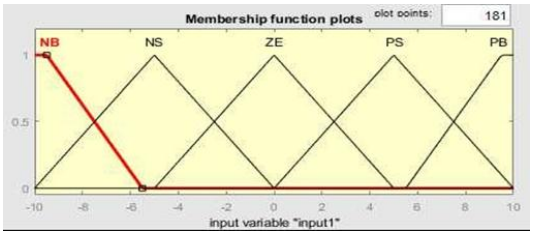

Fig 5. Membership Function of power Error

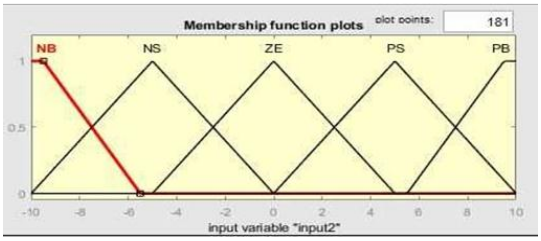

Fig 6. Membership Function of Change in power error

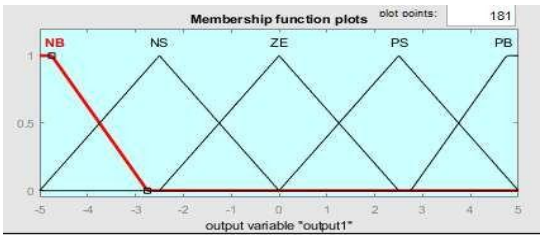

Fig 7. Membership Function of output

(ii) Set of ambiguous guidelines: FLC-based power flow regulation based on error and its variation in power error.

e/ce	P	NS	Z	PS	P
N	Z	NS	N	N	N
NS	Z	NS	N	NS	N
Z	P	PS	Z	NS	N
PS	P	PS	PS	Z	NS
P	P	P	P	PS	Z

Table I: Rules Table

By using a rule base and taking into account both the measured changes in the error and the conditions of the error data, the power flow control is decided. The procedure is carried out by consulting Table 1, which includes the required instructions. The Minimum-Maximum function is used to calculate the output's degree of membership, which enables evaluation of the output's membership in each individual fuzzy set.

(iii) Fuzzy Inference System: The final fuzzy value from the previous phase is sent to the inference mechanism stage, where the Mamdani method is used to apply the Minimum-Maximum rule. The Fuzzy Logic Controller (FLC) uses the fuzzy rule-based approach to guide its decisions at this level. These fuzzy values are processed by the FLC before being sent to the defuzzification procedure for additional examination and transformation into crisp values.

(iv) Defuzzification: In this stage, the centroid approach is used to convert the fuzzy values produced from the fuzzy inference mechanism into crisp values, more especially current values. The crisp output value is precisely represented using the centroid technique, which determines the fuzzy output membership function's centre of gravity. The acquired current values can be used for further analysis and control in the power flow system thanks to this conversion.

6. Representation of Maximum Power Point Tracking (MPPT) for Integrated Generator Rectifier System.

The MPPT method is used by the integrated generator rectifier system to monitor the peak power point. This study selects the Power Signal Feedback control approach from a range of alternatives. To maximise power extraction, it continuously monitors the power signal and modifies the operating point. It seeks to track the maximum power point and enhance system performance by utilising feedback loops. The peak power point is tracked via the power block diagram. The alignment of the obtained power with the peak power curve demonstrates successful MPPT at each generator speed.

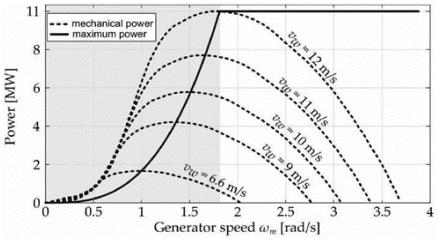

Fig 8. Illustration of maximum power curve as well as the mechanical power curves of an 11 MW wind turbine.

A graph of power curves at various wind speeds is shown. The mechanical power curves' peak points are connected to create the maximum power curve, which has a maximum power of 11 MW.

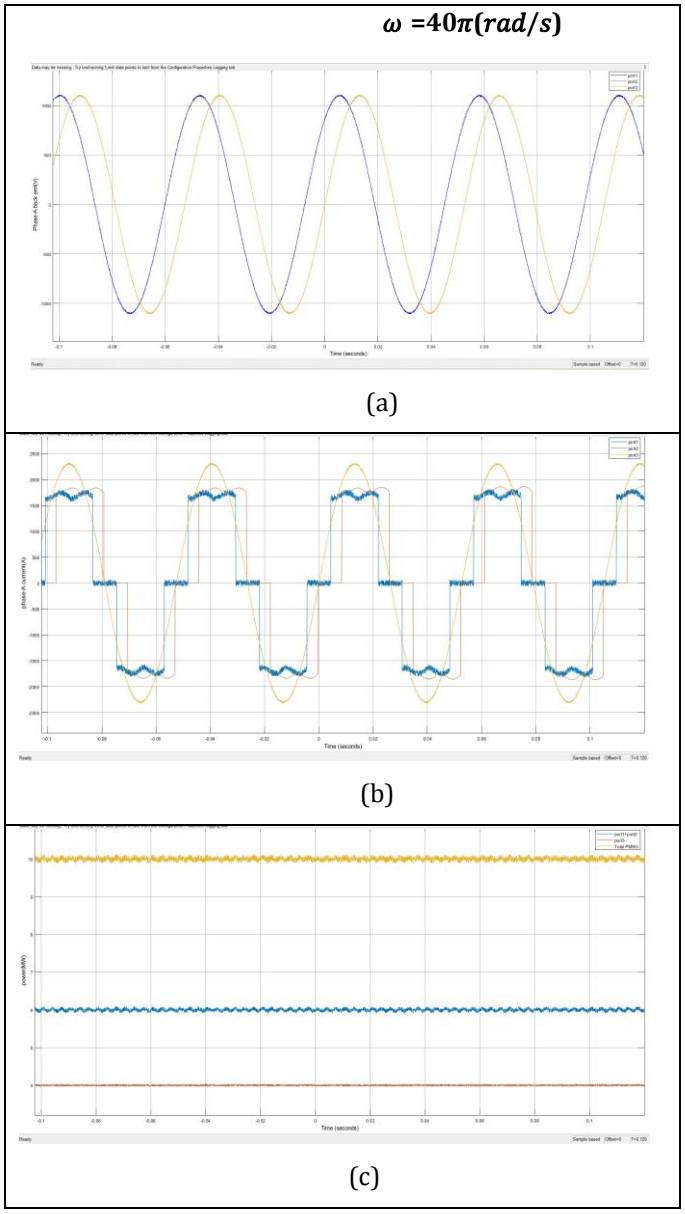

7. Simulation Results:

7.1 Controlling of Power Flow:

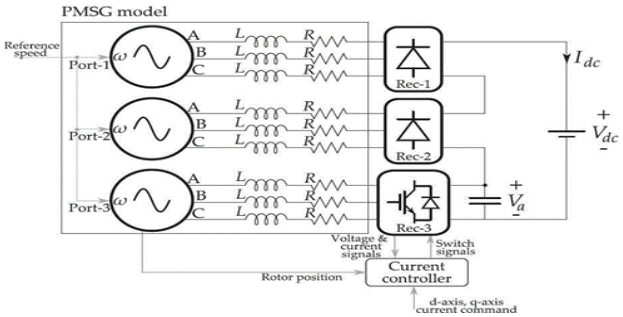

Fig 9. Three-port Permanent Magnet Synchronous Generator simulation model

The relationship between the d-axis current and the DC-bus power, which includes the power electronics switching circuits, as described in equation (6), is illustrated by the simulation model in Figure 9. Three voltage sources linked in series with a resistance (R) and an inductance (L) make up the three-port PMSG theoretically. An external speed reference signal determines the voltage sources' frequency (f) and amplitude (a). Connected to Ports I and II are uncontrolled three-phase diode rectifiers. To lessen voltage ripple in the DC outputs of the passive rectifiers, the phase-A (and phase-B and phase-C) voltages are phase-shifted by /6 electrical radian. Port-III is connected to active rectifiers, which are made up of IGBTs with a 2 kHz switching frequency. A DC bus is created by connecting the rectifier outputs in series. The grid connection is indicated by the DC bus voltage of 5.7 kV.

7.2 Maximum Power Point Tracking of DC-Bus Power:

For MPPT control, the simulation model in Figure 9 is used. The generator provides the reference speed for the wind turbine, represented by the symbol m.

$$J\omega_m \frac{d\omega_m}{dt} = P_{\text{turbine}} - P_{\text{dc}}$$

The wind turbine's moment of inertia, denoted as J, has a value of 28.7 × 10^6 $kg \cdot m$^2. In order to speed up simulation, the chosen value of J is 50 times smaller for simulation reasons [11].

The Phase-A back EMFs of Ports 1, 2, and 3 at the specified electrical frequency of 20 Hz are shown in Fig. 10(a). The Phase-A currents of the three AC ports for an 11 MW rated DC bus power are displayed in Fig. 10(b). Figure 10(c) illustrates the overall input power of the PMSG, which was calculated by adding the power outputs of all the back EMFs. Similar values at the lowest operating speed are shown in Figs. 10(d), (e), and (f). When comparing the two speeds at w = 40 (rad/s) and w = 22 (rad/s), it can be seen that the ripple factor gets smaller as the PMSG's overall power rises. The obtained ripple factor is below the permitted threshold.

Fig. 10 At $\omega = 40\pi(rad/s)$ the simulation waveforms are as follows**: (a)** At the rated speed of the generator, sinusoidal and phase-shifted back EMFs are observed. **(b)** The respective currents of phase-A are shown. **(c)** At the rated speed, the PMSG distributes input power between the active and passive rectifiers.

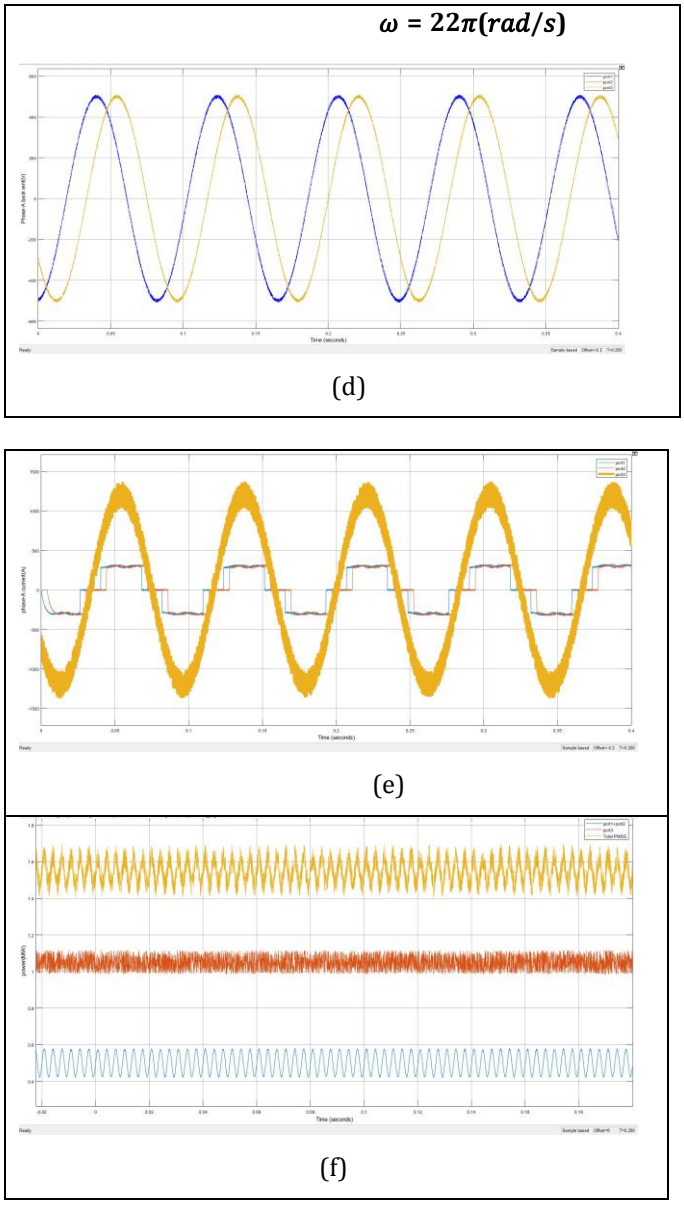

Fig.10 presents the simulation waveforms at $\omega = 22\pi(rad/s)$ as follows:**(d)** At the minimum operating speed, the back EMFs are equal to 55% of the rated speed back EMFs. **(e)** At the minimum operating speed, the phase-A currents exhibit specific patterns.

(f) At the minimum operating speed, the input power of the PMSG is shared between the active and passive rectifiers.

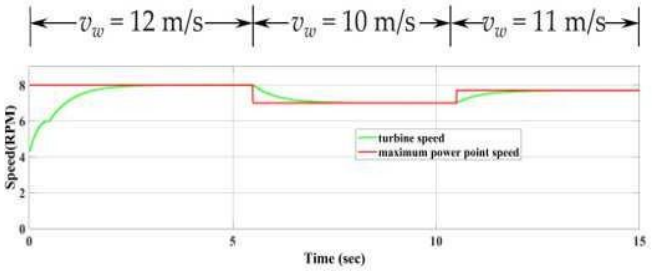

11.(a)

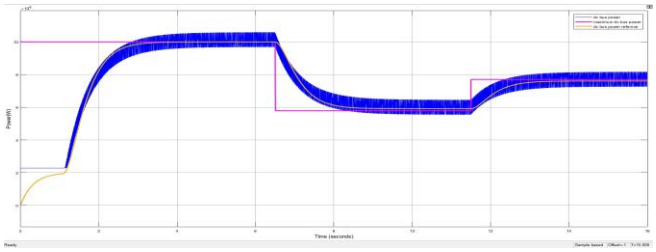

11.(b)

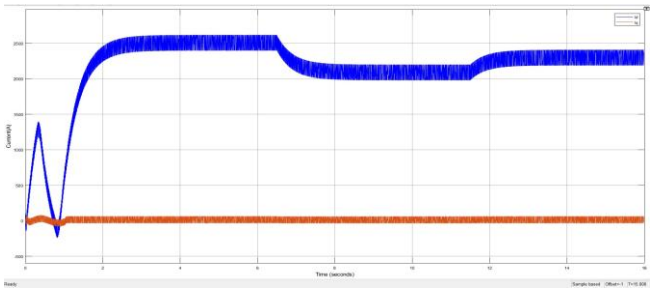

11.(c)

Fig.11 illustrates the waveforms demonstrating the MPPT capabilities of the system:**(a)** At each wind speed, the turbine speed (solid blue line) follows the optimal speed to generate maximum power.**(b)** The power of the DC bus and the mechanical power of the turbine are plotted against time, showing their relationship.

When the wind speed reaches 12 m/s, the turbine begins to spin at 55% of its rated speed. While the turbine's maximum output is 11 MW at this speed, the DC bus power is just 2 MW. According to Fig. 10(b), the MPPT algorithm modifies the turbine speed to generate the most power at 11 MW. The currents moving along the d-axis and q-axis are depicted in Fig. 10(c).The speed, power, and current curves at various wind speeds are depicted in Fig. 11. Fig.11(a) depicts the curves at a wind speed of 12 m/s, Fig.11(b) depicts the curves at a wind speed of 10 m/s, and Fig.11(c) depicts the curves at a wind speed of 11 m/s.

8. Conclusion:

For an integrated system integrating generators and rectifiers, a Fuzzy Logic Controller (FLC) based MPPT technique is suggested in this work. The maximum power point tracking (MPPT) of the system may be negatively impacted by the presence of passive rectifiers, which in turn impacts the levelized cost of energy. A new control strategy is developed to handle this problem, consisting of an FLC and power controller in the outer loop and a PI current controller with a feedback term in the inner loop. The Fuzzy Logic-based MPPT approach modifies the combined system's power signal to make sure that the DC bus power tracks the reference power, maximising the amount of energy that can be extracted from the wind. According to the results of the simulation, using a fuzzy controller improves levelized electricity costs by decreasing back electromotive force (EMF) ripples while also increasing maximum power obtained.

References:

i. P. T. Huynh, P. J. Wang, and A. Banerjee, “An integrated permanent magnet synchronous generator rectifier architecture for limited speed range applications,” IEEE Trans. Power Electron., vol. 35, no. 5, pp. 4767– 4779, May. 2020.

ii. P. Huynh and A. Banerjee, “Active voltage-ripple compensation in an integrated generator-rectifier system,” inProc. IEEE Appl. Power Electron. Conf. Expo., Mar. 2019, pp. 3199–3206.

iii. N. Celanovic and D. Boroyevich, “A comprehensive study of neutral- point voltage balancing problem in three-level neutral-point-clamped voltage source PWM inverters,” IEEE Trans. Power Electron., vol. 15, no. 2, pp. 242–249, Mar. 2000.

iv. GE Renewable Energy, “Haliade-X 12 MW offshore wind turbine platform,” Sep. 19, 2019. [Online]. Available: https://www.ge.com/ renewable energy/wind-energy/offshore-wind/haliade-x-offshore turbine.

v. V. Yaramasu, B. Wu, P. C. Sen, S. Kouro and M. Narimani, "High- power wind energy conversion systems: State-of-the-art and emerging technologies," in Proceedings of the IEEE, vol. 103, no. 5, pp. 740- 788, May 2015.